DYNAMICS AND ANALYSIS OF VORTEX-FLAME INTERACTION IN SWIRLING COMBUSTION FLOWS

Chris Stone*
and
Suresh Menon†
School of Aerospace Engineering,
Georgia Institute of Technology,
Atlanta, Georgia 30332,
suresh.menon@ae.gatech.edu

ABSTRACT

Large-Eddy Simulation (LES) methodology has been used to model combustion dynamics in a realistic swirling flow dump combustor. The effects of upstream velocity swirl on the combustion dynamics is investigated. A premixed flamelet model is employed to capture the interaction of the flame-front with the large-scale flow structures. It is observed that higher inlet swirl increases the overall stability of the combustion system. In addition to decreased pressure oscillations, the higher swirl reduced the flame-front oscillations and mean flame length.

INTRODUCTION

Due to the increasing emission regulations, low-NO_x gas turbines (LNGT) employing lean, premixed combustion are in high demand. Lean, premixed combustion results in the suppression of thermal NO_x formation due to the reduction in flame temperature (Zeldovich NO_x mechanism). However, as the lean blowout limit (LBO) is approached, the sensitivity to small perturbations in fuel concentration, flow velocity, temperature, and pressure increases. Under certain conditions, these fluctuations can be amplified, resulting in high-amplitude pressure oscillations. If not controlled and suppressed, these pressure fluctuations may lead to structural fatigue or even system failure.

At the heart of combustion dynamics is the coupling between the heat release and the pressure oscillations in the combustor. Accurate prediction of the effects of such coupling is especially difficult due to the unsteadiness of the driving processes (e.g., fuel injection) and the high nonlinearity of the interactions between turbulent mixing, acoustic wave propagation, and unsteady heat release. Large-scale flow structures play a key role in the coupling process by controlling the mixing of the essential ingredients of combustion: oxidizer, fuel, and heat. Realizing this, attempts have been made to control the vorticity both passively and actively.

Active control of instabilities through fuel modulation (Zinn and Neumeier, 1996) and flow control (Paschereit *et al.*, 1998) have been demonstrated in the past. Passive control using sudden expansions or bluff-bodies has also been conducted but these studies predominately focused upon axisymmetric flow instability, characteristic of non-swirling flows. Swirl stabilized combustion is quite common in gas turbine combustors; however, it has been reported by Sivasegaram and Whitelaw (1991) that swirl may drive instabilities in suddenly expanded flows. Unlike predominately two-dimensional flows, azimuthal (helical) instability modes may be important in highly swirling flows. Recently, experimental and numerical studies have been conducted on highly swirling combustion flows (Paschereit *et al.*, 1999; Kim *et al.*, 1999).

In order to control swirl-enhanced instabilities, it is vital to understand the large-scale dynamics of these complex, turbulent flows. However, the harsh conditions inside the combustion system make experimental studies difficult and expensive. By accurately simulating the governing fluid physics, numerical modeling of such systems can lead to a more detailed understanding of the combustion processes. For this study, Large-Eddy Simulations (LES) method has been used to model the combustion dynamics of a realistic combustion system. In addition to basic flow dynamics, vortex-flame interactions and their role in the dynamics is investigated.

*Graduate Research Assistant
†Professor

NUMERICAL MODEL

The LES equations of motion are solved on a three dimensional, boundary-conforming, finite-volume grid using MacCormack's explicit scheme (MacCormack, 1969). For brevity, the LES equations and numerical details are withheld but can be found elsewhere (Menon *et al.*, 2001). No-slip, adiabatic wall conditions conditions are used with non-reflecting inflow/outflow boundary conditions following Poinsot and Lele (1992). Clustering is employed near walls and in shear layer region to better resolve large scale fluctuations.

To increase simulation turn-around time, the computational domain is evenly distributed in parallel using the Message-Passing Interface (MPI) standard. An advantage of the explicit scheme used here is the ease of load balancing since every cell requires the same amount of work resulting in high parallel efficiency.

A cylindrical dump combustor consisting of an inlet pipe expanding into the larger combustion zone is simulated. A rendering of the combustor and computational grid is shown in Figure 1. For this study, a cylindrical grid of 181 × 65 × 81 was employed. The ratio of combustor diameter (D_c) to inlet diameter (D_0) is 3.2. The inlet pipe is included to simulate the region downstream of a swirling premixer. Additionally, by including the inlet, natural flow instabilities are allowed to form upstream of the dump plane. The mean inlet mass flow rate, temperature, and pressure are 0.435 Kilograms/second, 673 Kelvin, and 11.8 atmospheres, respectively. The Reynolds number based on inlet bulk velocity and inlet diameter is 527,000. An inflow turbulent field is generated by using a specified turbulence intensity (7%) on a randomly generated Gaussian field. The fuel and air at the inflow is assumed to be perfectly premixed. To wash out the effects of the initial conditions the simulations are allowed to run several flow-through-times before any data is collected for analysis.

To excite acoustic resonance and accelerate the exiting flow, a 60% convergence is placed at the outflow; however, the flow remains subsonic. It must noted that this sub-sonic condition is not the perfect pressure boundary obtained had the outflow been choked.

Premixed Combustion Model

Due to the high expense and numerical difficulties of finite-rate chemistry, the premixed combustion is modeled with a G-equation flamelet formulation (Smith and Menon, 1996). In this model, a progress variable G is defined such that $G = 1$ for the reactant gas and $G = 0$ for the products. Upon filtering, the G-equation takes the following form,

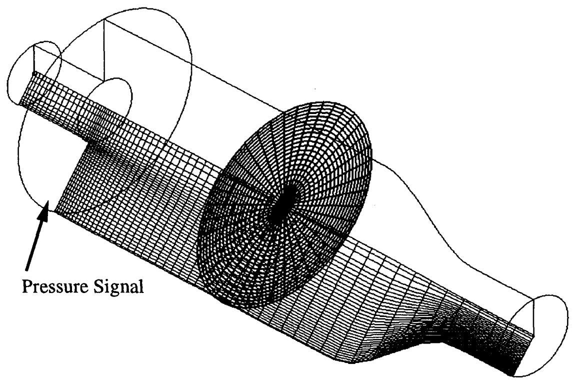

Figure 1: Geometry and computational grid (181 × 65 × 81) employed in this study (showing only every third grid point). Pressure signal is recorded at the base of the combustor.

$$\frac{\partial \bar{\rho}\tilde{G}}{\partial t} + \nabla \cdot \bar{\rho}\tilde{u}\tilde{G} = -S^{sgs} - \nabla \cdot G^{sgs}, \qquad (1)$$

where $\bar{\rho}$, $\tilde{G}$, $\tilde{u}$ are the filtered density, G, and velocity fields, respectively. The resulting subgrid terms which require modeling are the unresolved transport, $G^{sgs} = \bar{\rho}[\widetilde{uG} - \tilde{u}\tilde{G}]$, and the source term, $S^{sgs} = \overline{\rho_o S_L^o |\nabla G|}$. The density and laminar flame speed are both taken at some reference condition. The evolution of the progress variable is balanced by the fluid convection and flame-normal burning rate. Details of the reaction rates and molecular diffusion/conduction are contained in the laminar flame speed, S_L^o. The unresolved transport term is modeled with a gradient diffusion assumption and the source term is approximated as $S^{sgs} \approx \rho_o S_t |\nabla \tilde{G}|$. Here, S_t, is the local turbulent flame speed averaged over a characteristic LES length cell. For the present study, Pocheau's flame speed model (Pocheau, 1994) has been used to determine the turbulent flame speed in the following form;

$$\frac{S_t}{S_L} = (1 + \beta \frac{u'^{\alpha}}{S_L^{\alpha}})^{\frac{1}{\alpha}}. \qquad (2)$$

Here, $\alpha = 2$ for energy conservation and β is an adjustable parameter set to 20 (Kim *et al.*, 1999).

Recently, a closure for S_t, known as the *broadened flame model*, has been developed by Kim and Menon (Kim and Menon, 2000) which uses dynamically evaluated turbulence quantities (Localized Dynamic K-equation Model, LDKM). This model allows the simulation of flames in the *thin-reaction-zones regime* over a wide range of turbulence levels. We will investigate such a model and its impact on the combustion dynamics in the future.

RESULTS

For this study, two simulations were conducted in order to observe the effects of inlet swirl on the dynamics in the combustor. The two cases, from here on referred to as Cases A and B, have the same conditions except for different inlet swirling velocity profiles. A non-dimensional Swirl number, S, can be defined as:

$$S = \frac{\int_0^R \rho u w r^2 \mathrm{d}r}{R \int_0^R \rho u^2 r \mathrm{d}r}, \qquad (3)$$

where R is the inlet pipe radius. The Swirl number at the inlet pipe entrance, S_i, is 0.56 and 1.12 for Case A and B, respectively. For both Cases, the specified flame temperature, T_{flame}, is 1811.0 Kelvin.

Despite the high S_i imposed at the inlet, the swirl number at the dump plane is lower due to the convection through the inlet pipe. The swirl numbers based on the time-averaged velocity data at the dump plane for Case A and B are, respectively, 0.4 and 0.71. The three component velocity profiles (U_x, U_r, U_θ) at the dump plane are shown in Figure 2. As can be seen, U_x resembles a plug flow profile for S_i = 0.56, while the centerline velocity is significantly lower in Case B.

As previously stated, swirling flow is often used as a stabilizing mechanism in conjunction with sudden expansions in most combustion devices. This is due to the reduction in the axial velocity through the dump plane as the streamlines expand radially. If the Swirl and Reynolds numbers are large enough, a recirculation zone can be formed along the combustor centerline (Dollenback *et al.*, 1988). Figure 3 shows the mean axial velocity (U_x / U_0) profiles for both cases. As can been seen, the axial velocity is significantly decreased in the presence of the higher inlet swirl. Further downstream, the axial velocity is actually stagnated but the higher swirl, i.e., recirculation occurs.

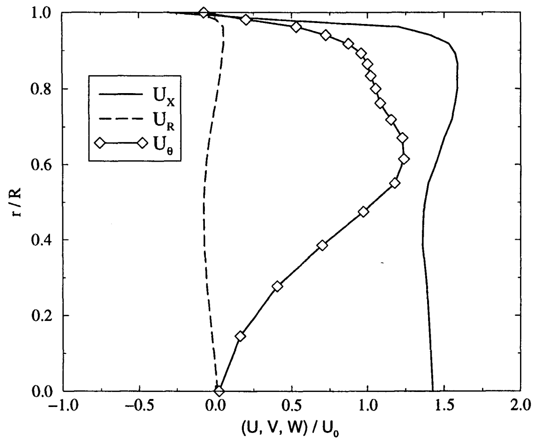

(a) Case A: S_i = 0.56

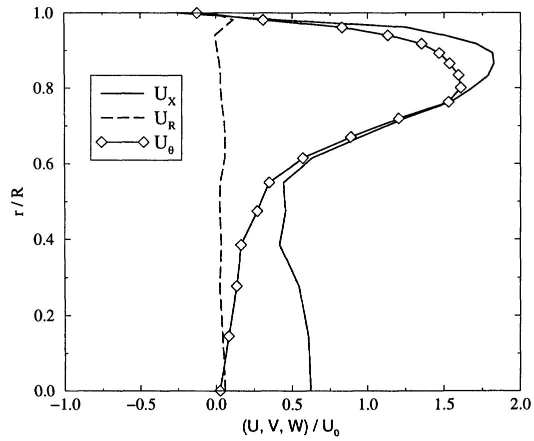

(b) Case B: S_i = 1.12

Figure 2: Mean axial, radial, and azimuthal velocity (U_x, U_r, U_θ) profiles at the dump plane. Radial distance is non-dimensionalized by itself and all velocities are referenced to U_0.

The effects of the swirl on the mean velocity profile are clearly evident in the Figure 4. There, the stream-wise mean axial velocity contours are shown. The top half of the figure shows the contours from Case A while the bottom half shows Case B. As can be seen, the shear layer spreads much faster with the higher swirl.

As a consequence of the reduced centerline velocity, the swirl stabilized flame is shortened for Case B. Plotted in Figure 5 is the centerline profile of the non-dimensional temperature, Θ defines as $\Theta = (\overline{T} - T_0) / (T_{flame} - T_0)$. In this context, Θ represents the mean flame front and gives an indication of the mean flame length. As can be seen, the temperature profile for Case B is much steeper and the flame tip is held closer to the dump plane. Since a thin-flame

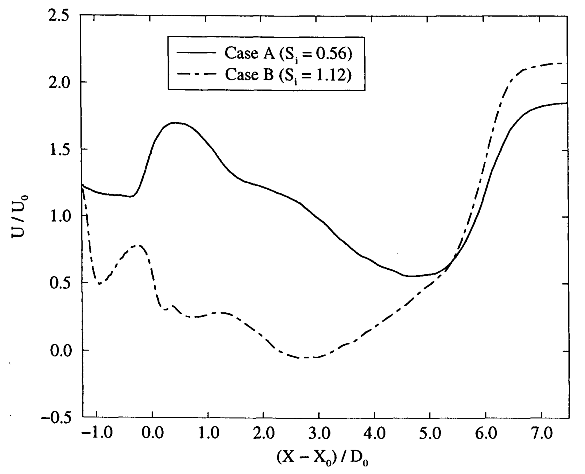

Figure 3: Mean axial velocity ($\overline{U}$ / U_0) along centerline. Lengths are non-dimensionalized by inlet pipe diameter, D_i.

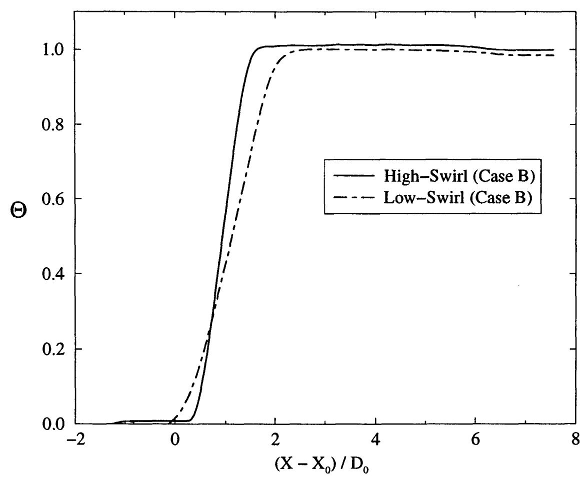

Figure 5: Centerline temperature (non-dimensional) profile for both cases.

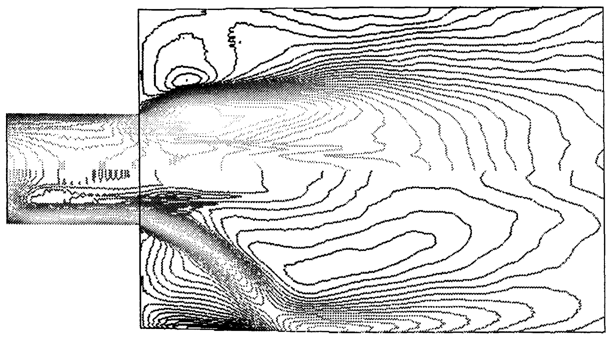

Figure 4: Mean axial velocity contours. Top half of the figure is from Case A and bottom is Case B. The data from Case B is taken at the same azimuthal location as Case A ($\theta = 0^o$) but is transposed to add in the visualization.

model is being used for this study, the lower temperature profile indicates that the flame is moving more in the axial direction of Case A (pulsing in time).

Shown in Figure 6(a) is the pressure fluctuation spectra. The pressure signals were recorded at the base of the dump plane (see Figure 1) where the vorticity is believed to be low. Case A shows a dominant frequency (plus higher harmonics) at a Strouhal number (defined as $f\ D_0/U_0$) of 1.12 (2.24, 3.36, etc. for the harmonics). For Case B, the peak frequency shifted to 1.84. It should be noted that no harmonics of any significant power were observed. To discern the nature of the observed pressure signal, the Fourier amplitudes from the 1.12 frequency have been calculated along the length of the combustor. The results of this are plotted in Figure 6(b). There, the wave shape corresponds to that of a 3/4 wave. Similar analysis of Case B did not reveal any wave shape indicating that the pressure fluctuations are not necessarily acoustic in nature (the fluctuating vorticity at the recorder location is higher for Case B compared to Case A).

A useful indication of the stability of a combustion system is the Rayleigh parameter, $R(x,t)$. $R(x,t)$ gives the correlation of the unsteady pressure fluctuations, p', with the unsteady heat release, $\Delta q'$. Positive $R(x,t)$ indicates pressure fluctuation amplification while a negative value corresponds to attenuation (or stable combustion). Following Menon (1992), the volume averaged Rayleigh parameter, $R(t)$ has been computed and the results from Case A are shown in Fig 7. This time segment reveals mostly negative $R(t)$. This indicates that the heat release fluctuations and the dominant pressure mode are in not phase. However, positive $R(t)$ is observed at the $St = 2.24$ harmonic.

As mentioned previously, the flame is shortened by the higher swirl. In addition to this, the flame structure is also altered. Presented in Figures 8(a) and (b), are the 3D instantaneous flame surfaces (ISO-surface of the instantaneous G field) and the instantaneous azimuthal vorticity (ω_θ) contours for both cases. For Case A (Figure 8(a)), distinct coherent structures are seen to propagate downstream from the dump plane. This coherent vortices (ring structures if view as an ISO-surface) entrain the flame surface and pull it downstream. The flame surface is stretched downstream until it eventually collapses and is pinched-off. This vortex-flame interaction causes a pulsation at the same $St = 1.12$ mode as the pressure oscillations (Fig 6). On the other hand, no coherent structures, such as those observed for Case A, are seen in Figure 8(b). Instead, a wide, cone-shaped shear layer is seen. The flame is highly

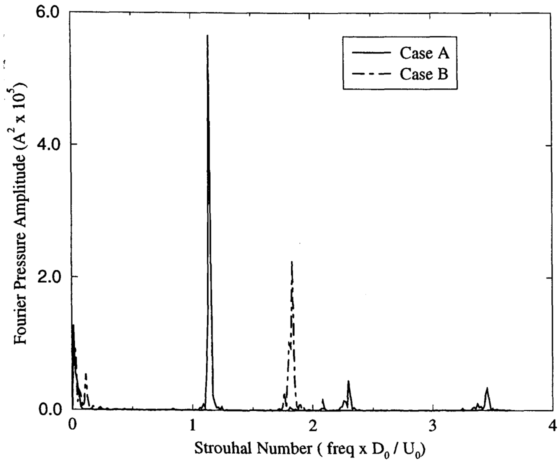

(a) Fourier Transform

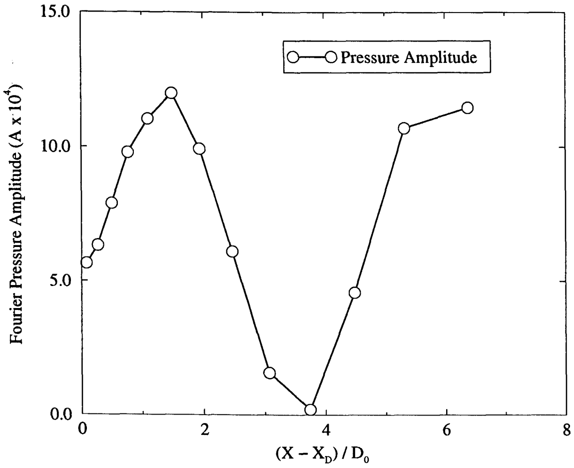

(b) Fourier Mode Analysis

Figure 6: (a) Fourier transform of the pressure fluctuations in the combustor and (b) Mode shape of the $St = 1.12$ frequency.

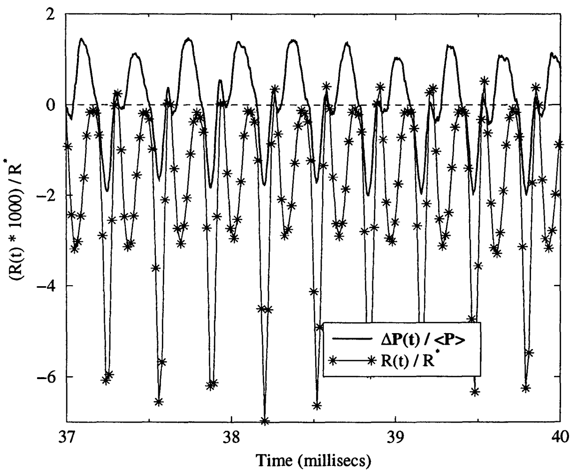

Figure 7: Time segment of the Volume average Rayleigh parameter, $R(t)$. Positive $R(t)$ corresponds to pressure fluctuation amplification.

strained and contorted yet it remains stationary. As a result, no pulsing phenomena is observed in Case B.

CONCLUSIONS

Large-Eddy Simulation methodology has been used to model combustion dynamics in a swirling dump combustor. The G-Equation premixed combustion model was used to simulate the flame propagation. To investigate the effects of inlet velocity swirl on the combustion dynamics, two simulations are conducted with different velocity profiles. For the lower swirl number simulation, a dominant standing acoustic wave formed along with its family of harmonics. Also, large-scale coherent structures were observed to entrain the flame surface and cause flame pulsation. It is observed that increased swirl reduced flame pulsation and pressure fluctuation amplitudes. As a result, the overall state of the combustion system was more stable. In addition to reduced pressure fluctuation amplitudes, the mean flame position was shorter.

ACKNOWLEDGEMENTS

This work was financially supported by General Electric Power Systems. High Performance Computing (HPC) resources provided by the Department of Defense (DOD) Major Shared Resources Centers (MSRC) at Naval Oceanographic Office (NAVOCEANO), Aeronautical Systems Center (ASC), and Army Engineering Research and Development Center (ERDC) under Army Research Office (ARO) and Wright-Patterson AFB HPC Grand Challenge Projects.

References

Dollenback, P. A., Metzger, D. E., and Neitzel, G. P., 1988, "Measurements in turbulent swirling flow through an abrupt axisymmetric expansion," *AIAA Journal*, Vol. 26, Num. 6, pp. 669-681.

Kim, W.-W., and Menon, S., 1999, "Numerical modeling of turbulent premixed flames in the thin-reaction-zones regime," *Combustion Science and Technology*, Vol. 160, pp. 110-150.

Kim, W.-W., Menon, S., and Mongia, H. C., 1999, "Large eddy simulations of a gas turbine combustor flow," *Combustion Science and*

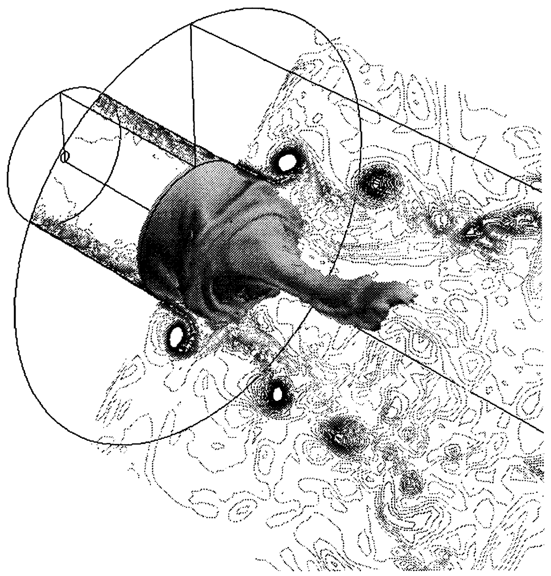

(a) Case A

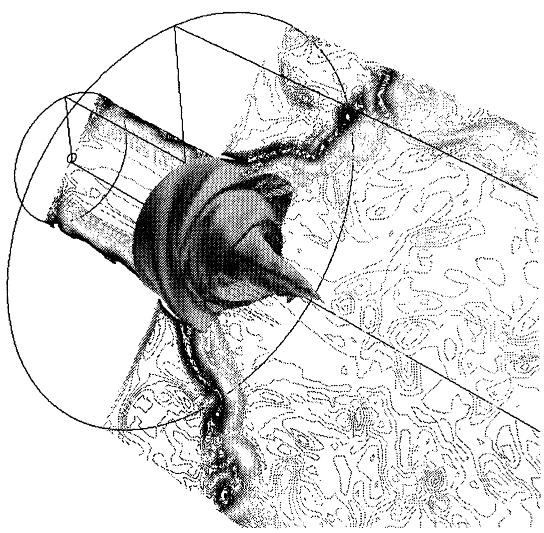

(b) Case B

Figure 8: Vorticity in the combustor

Technology, Vol. 143, pp. 25-62.

MacCormack, R. W., 1969, "The effects of viscosity in hyper-velocity impact cratering," *AIAA Paper 69-354*.

Menon, S., 1992, "Active combustion control in a ramjet using large-eddy simulations,", *Combustion Science and Technology*, Vol. 84, pp. 51-79.

Menon, S., Sankaran, V., Stone, C., and Sekar, B., 2001, "Dynamics of swirling premixed and spray flames," *AIAA-2001-1092*

Paschereit, C., Gutmark, E., and Weisenstein, W., 1999, "Coherent structures in swirling flows and their role in acoustic combustion control," *Physics of Fluids*, Vol. 11, pp. 2667-2678.

Pashereit, C. O., Gutmark, E., and Wolfgang Weisenstein, W., 1998, "Control of thermoacoustic instabilities and emissions in an industrial–type gas–turbine combustor," *Proceedings of the 27th International Symposium on Combustion*, pp. 1817-1824.

Pocheau, A., 1994, "Scale invariance in turbulent front propagation," *Physical Review E*, Vol. 49, pp. 1109-1122.

Poinsot, T. and Lele, S., 1992, "Boundary conditions for direct simulations of compressible viscous flow", *Journal of Computational Physics*, Vol. 101, pp. 104-129.

Sivasegaram, S., and Whitelaw, J., 1991, "The influence of swirl on oscillations in ducted premixed flames," *Combustion Science and Technology*, Vol. 85.

Smith, T. M. and Menon, S., 1996, "The structure of premixed flames in a spatially evolving turbulent flow," *Combustion Science and Technology*, Vol. 119, pp. 77-106.

Zinn, B., and Neumeier, Y., 1996, "Control of combustion instabilities with secondary fuel injection using real time modes observation: practical implementation," *Proceedings of the Combustion Institute, vol. 26, 1998.*